Influence of electromagnetic Field Damping on the Vibration Stability of soft mounted Induction Motors with Sleeve Bearings, based on a Multibody Model

U. Werner

The paper shows an analytical vibration model for stability analysis of soft mounted induction motors with sleeve bearings, especially focusing on the influence of electromagnetic field damping on the limit of vibration stability. The model is a multibody model, considering the electromagnetic influence – including the electromagnetic field damping effect –, stiffness and internal material damping of the rotor structure, stiffness and damping of the bearing housings and end shields, stiffness and damping of the foundation elements and stiffness and damping of the oil film of the sleeve bearings. The aim of the paper is to unite all these influences in a model and to derive a procedure for calculating the limit of vibration stability, with considering the electromagnetic field damping effect. Additionally, a numerical example is presented, where the influence of electromagnetic field damping on the limit of vibration stability is shown, as well as the influence of the foundation elements and of the internal damping of the rotor. The procedure and conclusions can also be adopted into finite-element analysis.

1 Introduction

For analyzing rotating machinery, it is important to know the limit of vibration instability, which is e.g. influenced by the oil film of the sleeve bearings and internal material damping of the rotor (rotating damping), described by Rao (1996), Gasch (2002) and Genta (2005). In electrical machines, also electromagnetic fields occur, which couple the rotor to the stator and influences the vibration behavior, described by Schuisky (1972), Früchtenicht et al. (1982), Seinsch (1992), Smith et al. (1996), Arkkio et al. (2000), Holopainen (2004) and Werner (2006). Especially in induction motors an electromagnetic field damping effect occurs, which itself influences the electromagnetic forces and therefore the vibration behavior, shown by Früchtenicht et al. (1982), Seinsch (1992), Arkkio et al. (2000), Holopainen (2004), Werner (2006) and Werner (2016). Sometimes large induction motors (1MW-10MW) with sleeve bearings and high speeds (3000 rpm-6000 rpm) are mounted on soft foundation elements (rubber elements) to decouple the motor from the foundation (Fig.1). However, a soft mounting influences the vibration behavior of the machine clearly, which is demonstrated by Kirk at al. (1974), Gasch et al. (1984) and Werner (2008).
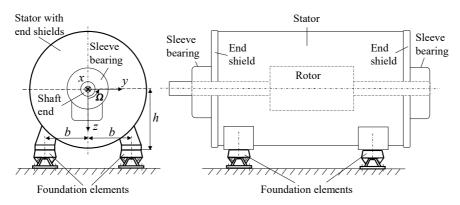

Figure 1. Soft mounted induction motor with sleeve bearings

Up to now, electromagnetic field damping of induction motors is often not considered for vibration analysis in the industry. Therefore the aim of the paper is now to present an analytical vibration model of a soft mounted induction motor with sleeve bearings and to derive a practicable method to consider the influence of electromagnetic field damping on the limit of vibration stability.

2 Electromagnetic Field Damping

An eccentricity $\hat{e}$ between the shaft centre point W of the rotor and the centre of the stator bore leads to additionally electromagnetic eccentricity fields, which cause a radial magnetic force $\hat{F}_{mr}$ in direction of the smallest air gap (Fig. 2a). If the rotor angular frequency Ω is different to the angular frequencies of the eccentricity fields, these fields induce voltage into the rotor cage, which reduces the magnitude of origin eccentricity fields. Therefore, the radial magnetic force $\hat{F}_{mr}$ will be reduced and an additional magnetic force $\hat{F}_{mt}$ in tangential direction is caused (Fig. 2a).
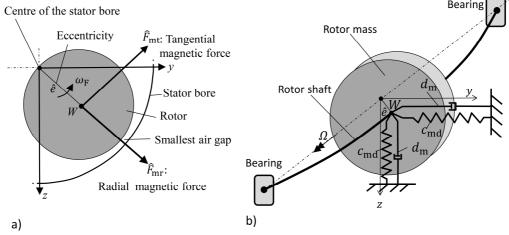

Figure 2. a) Electromagnetic forces; b) Magnetic spring and magnetic damper

The following equations are fundamentally based on the investigations of Früchtenicht et al. (1982) and Seinsch (1992). The radial magnetic force can be described by an electromagnetic spring element c_{md} (Fig. 2b):

$$p > 1: \quad c_{md} = \frac{c_m}{2} \cdot (\alpha_{p+1} + \alpha_{p-1}); \qquad p = 1: \quad c_{md} = c_m \cdot \alpha_{p+1} \tag{1}$$

Where p is the number of pole pairs of the motor, c_m electromagnetic spring element without electromagnetic field damping, and α_{p+1} and α_{p-1} are the real parts of the complex field damping value. Without electromagnetic field damping, the real parts of the field damping coefficients get $\alpha_{p+1} = \alpha_{p-1} = 1$. For 2-pole motors ($p = 1$) the component α_{p-1} gets zero, neglecting the homopolar flux.

$$p > 1: c_m = \frac{\pi \cdot R \cdot l}{2 \cdot \mu_0 \cdot \delta''} \cdot \hat{B}_p^2 \; ; \qquad p = 1: \quad c_m = \frac{1}{2} \cdot \frac{\pi \cdot R \cdot l}{2 \cdot \mu_0 \cdot \delta''} \cdot \hat{B}_p^2 \tag{2}$$

Where R is the radius of the stator bore, l is the length of the core, μ_0 is the permeability of air, δ'' is the equivalent magnetic air gap width – depending on mechanical air gap, saturation effects and CARTER-factors, described by Seinsch (1992) –, $\hat{B}_p$ is the amplitude of fundamental air gap field. The tangential magnetic force can be described by the electromagnetic damper element d_m (with $\omega_F \neq 0$) (Fig. 2b):

$$p > 1: d_m = -\frac{1}{\omega_F} \cdot \frac{c_m}{2} \cdot (\delta_{p+1} - \delta_{p-1}); \qquad p = 1: \quad d_m = -\frac{1}{\omega_F} \cdot c_m \cdot \delta_{p+1} \tag{3}$$

Where ω_F is the whirling angular frequency of the rotor and δ_{p+1} and δ_{p-1} are imaginary parts of the complex field damping value. Without electromagnetic field damping, the field damping coefficients get $\delta_{p+1} = \delta_{p-1} = 0$. For 2-pole motors ($p = 1$) the component δ_{p-1} gets also zero, neglecting the homopolar flux. If electromagnetic field damping has to be considered, the electromagnetic field damping coefficients $\alpha_{p+1}, \alpha_{p-1}, \delta_{p+1}, \delta_{p-1}$ have to be derived. With the ordinal number $v = p \pm 1$ for an eccentricity field wave, the electromagnetic field damping coefficients can be calculated:

$$\alpha_v = 1 - K_v \cdot s_v^2 \; ; \quad \delta_v = -K_v \cdot \beta_v \cdot s_v \tag{4}$$

$$\text{with: } \beta_v = \frac{R_{2,v}}{\omega_1 (L_{2h,v} + L_{2\sigma,v})} \quad \text{and } K_v = \frac{1}{\beta_v^2 + s_v^2} \cdot \frac{\xi_{Schr,v}^2 \cdot \zeta_{K,v}^2}{1 + \frac{L_{2\sigma,v}}{L_{2h,v}}}$$

Where $R_{2,v}$ is the resistance of a rotor bar and ring segment, ω_1 is the electrical stator angular frequency, $L_{2h,v}$ is the main field inductance of a rotor mesh, $L_{2\sigma,v}$ is the leakage inductance of a bar and ring segment, $\xi_{Schr,v}$ is the screwing factor and $\zeta_{K,v}$ is the coupling factor, which are all described in detail by Seinsch (1992).

The harmonic slip s_v can be described by:

$$s_v = \frac{\frac{\omega_v}{v} - \Omega}{\frac{\omega_1}{v}} \quad \text{with:} \quad \Omega = \frac{\omega_1}{p}(1-s) \tag{5}$$
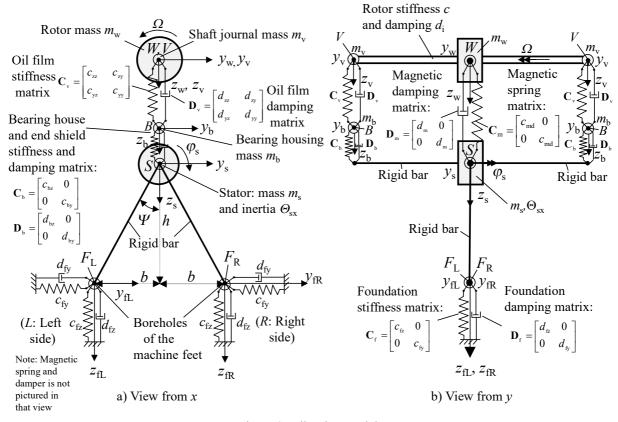
Where s is the fundamental slip of the induction motor, ω_1 is the electrical stator angular frequency and ω_v/v are the angular frequencies of the eccentricity fields, depending on the kind of eccentricity:
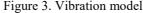
- Static eccentricity: $\omega_v = \omega_1$
- Dynamic eccentricity as a circular forward whirl: $\omega_v = \omega_1 \pm \omega_F$
- Dynamic eccentricity as a circular backward whirl: $\omega_v = \omega_1 \mp \omega_F$

To consider the electromagnetic field damping effect by a magnetic spring element c_{md} and by a magnetic damper element d_m, the compromise has to be made, that the calculation of c_{md} and d_m is here only based on circular forward whirls. With this simplification, the electromagnetic influence is supposed to be higher than it maybe in reality. If the absolute value of the harmonic slip $|s_v|$ is high – as it is for a circular backward whirl in conjunction with a small fundamental slip s – which is usual for steady state operation – the damped magnetic spring c_{md} gets very small as well as the magnetic damper d_m. In this case, the eccentricity fields induce strongly in the rotor cage and so the eccentricity fields get clearly reduced due to the harmonic rotor currents. Therefore, calculating c_{md} and d_m based on circular forward whirls presents the worst case regarding the height of the electromagnetic influence, when considering electromagnetic field damping, shown by Werner (2016).

3 Vibration Model

The model is an enhancement to the model, described by Werner (2008), where no electromagnetic field damping has been considered, no internal damping of the rotor, and no damping of bearing housings and end-shields. The vibration model is a simplified plane vibration model (plane y, z). It consists of two main masses, the rotor mass m_w, concentrated in the shaft centre point W, and the stator mass m_s, which has the inertia θ_{sx} and is concentrated in the centre of gravity S (Fig. 3).

Figure 3. Vibration model

Additional masses are the mass of the shaft journal m_v and the mass of the bearing housing m_b, which are accounted separately, mostly to avoid zeros at the main diagonal of the mass matrix. Due to their low mass, their influence is only marginal. The rotor rotates with the rotary angular frequency Ω. The inertia moments of the

rotor are not considered and therefore also no gyroscopic effects. The shaft journal centre point V describes the movement of the shaft journal in the sleeve bearing. The point B is positioned in the axial middle of the sleeve bearing shell and describes the movement of the bearing housing. The rotor mass is linked to the stator mass by the stiffness c and internal damping d_i of the rotor, the oil film stiffness matrix $\mathbf{C}_v$ and oil film damping matrix $\mathbf{D}_v$ of the sleeve bearings, which are supposed to be equal for the drive side and the non-drive side, and the bearing house and end shield stiffness and damping matrix $\mathbf{C}_b$ and $\mathbf{D}_b$, which are also assumed to be equal for the drive side and the non-drive side. The stator structure is assumed to be rigid, compared to the soft foundation. The foundation stiffness matrix $\mathbf{C}_f$ and the foundation damping matrix $\mathbf{D}_f$ connect the stator feet, F_L (left side) and F_R (right side), to the ground. The foundation stiffness and damping on the right side is the same as on the left side and the foundation stiffness values c_{fy} and c_{fz} and the foundation damping values d_{fy} and d_{fz} are the values for each motor side. The electromagnetism is considered by the electromagnetic spring and damper matrix $\mathbf{C}_m$ and $\mathbf{D}_m$, where also electromagnetic field damping is included. All used coordinate systems are fixed.

For deriving the damping coefficients, it is important to consider here, that natural vibrations with the angular natural frequency ω_{stab} of the critical mode at the limit of stability with the rotary angular frequency Ω_{stab} has to be analyzed. Therefore the whirling frequency ω_F becomes ω_{stab}:

$$\omega_F = \omega_{stab} \tag{6}$$

The oil film stiffness and damping coefficients c_{ij} and d_{ij} ($i, j = z, y$) of the sleeve bearing are calculated by solving the Reynolds differential equation, shown by Tondl (1965), Glienicke (1966) and Lund et al.(1987).

$$c_{ij} = c_{ij}(\Omega) \text{ and } d_{ij} = d_{ij}(\Omega) \tag{7}$$

Referring to Gasch (2002), the internal material damping of the rotor d_i is described here by the mechanical loss factor $\tan\delta_i$ of the rotor, depending on the whirling angular frequency ω_F.

$$d_i(\omega_F) = \frac{c \cdot \tan\delta_i}{\omega_F} \tag{8}$$

With the stiffness of the bearing housing and end shield (c_{bz}; c_{by}), the damping of the bearing housing and end shield (d_{bz}; d_{by}) is here also described by the mechanical loss factor $\tan\delta_b$:

$$d_{bz}(\omega_F) = \frac{c_{bz} \cdot \tan\delta_b}{\omega_F} \; ; \quad d_{by}(\omega_F) = \frac{c_{by} \cdot \tan\delta_b}{\omega_F} \tag{9}$$

The damping of the foundation elements is also described by the mechanical loss factor $\tan\delta_f$:

$$d_{fz}(\omega_F) = \frac{c_{fz} \cdot \tan\delta_f}{\omega_F} \; ; \quad d_{fy}(\omega_F) = \frac{c_{fy} \cdot \tan\delta_f}{\omega_F} \tag{10}$$

The electromagnetic stiffness coefficient c_{md} and damping coefficient d_m are depending on the harmonic slip s_v, and therefore also depending on the whirling angular frequency ω_F (see chapter 2).

$$c_{md} = c_{md}(\omega_F) \text{ and } d_m = d_m(\omega_F) \tag{11}$$

4 Mathematical Description

To calculate the limit of stability, it is necessary to derive the homogenous differential equation. Therefore, d'Alemberts method is applied to the vibration system in order to derive the equations of motion, leading to the parts: a) rotor mass system, b) journal system, c) bearing house system and d) stator mass system – (Fig. 4).

Because of the small displacements of the stator mass (z_s, y_s, φ_s), compared to the dimensions of the machine (h, b, Ψ), following linearization is possible: The machine feet displacements on the left side (z_{fL}, y_{fL}) and the machine feet displacements on the right side (z_{fR}, y_{fR}) can be described by the displacements of the stator (z_s, y_s, φ_s) by:

$$z_{fL} = z_s - \varphi_s \cdot b; \quad z_{fR} = z_s + \varphi_s \cdot b; \quad y_{fL} = y_{fR} = y_s - \varphi_s \cdot h \tag{12}$$

With the equilibrium of at each single system, the homogenous differential equation can be derived:

$$\mathbf{M} \cdot \ddot{\mathbf{q}} + \mathbf{D} \cdot \dot{\mathbf{q}} + \mathbf{C} \cdot \mathbf{q} = \mathbf{0} \tag{13}$$

Coordinate vector $\mathbf{q}$:

$$\mathbf{q} = \left[z_s; z_w; y_s; y_w; \varphi_s; z_v; z_b; y_v; y_b \right]^T \tag{14}$$

Rotor mass system

$$d_m(\dot{z}_w - \dot{z}_s) + d_i(\dot{z}_w - \dot{z}_v)$$
$$c(z_w - z_v) + \Omega \cdot d_i(y_w - y_v)$$
$$m_w \cdot \ddot{y}_w \qquad m_w \cdot \ddot{z}_w$$

$$c_{md}(y_w - y_s)$$

$$d_m(\dot{y}_w - \dot{y}_s) + d_i(\dot{y}_w - \dot{y}_v)$$
$$c(y_w - y_v) - \Omega \cdot d_i(z_w - z_v)$$

$$c_{md}(z_w - z_s) \qquad \text{a)}$$

Bearing house system

$$d_{bz}(\dot{z}_b - \dot{z}_s)$$
$$c_{bz}(z_b - z_s)$$
$$m_b \cdot \ddot{z}_b$$

$$c_{by}(y_b - y_s) \qquad c_{yz}(z_v - z_b) + c_{yy}(y_v - y_b) +$$
$$+ d_{yz}(\dot{z}_v - \dot{z}_b) + d_{yy}(\dot{y}_v - \dot{y}_b)$$

$$d_{by}(\dot{y}_b - \dot{y}_s) \quad m_b \cdot \ddot{y}_b$$

$$c_{zz}(z_v - z_b) + c_{zy}(y_v - y_b) +$$
$$+ d_{zz}(\dot{z}_v - \dot{z}_b) + d_{zy}(\dot{y}_v - \dot{y}_b) \qquad \text{c)}$$

Journal system

$$c_{zz}(z_v - z_b) + c_{zy}(y_v - y_b) +$$
$$+ d_{zz}(\dot{z}_v - \dot{z}_b) + d_{zy}(\dot{y}_v - \dot{y}_b)$$

$$m_v \cdot \ddot{y}_v \quad m_v \cdot \ddot{z}_v \quad \frac{d_i}{2}(\dot{y}_w - \dot{y}_v)$$

$$c_{yz}(z_v - z_b) + c_{yy}(y_v - y_b) + \qquad \frac{c}{2}(y_w - y_v) - \frac{\Omega \cdot d_i}{2}(z_w - z_v)$$
$$+ d_{yz}(\dot{z}_v - \dot{z}_b) + d_{yy}(\dot{y}_v - \dot{y}_b) \quad \frac{d_i}{2}(\dot{z}_w - \dot{z}_v)$$

$$\frac{c}{2}(z_w - z_v) + \frac{\Omega \cdot d_i}{2}(y_w - y_v) \qquad \text{b)}$$

Stator mass system

$$c_{md}(z_w - z_s)$$
$$m_s \cdot \ddot{z}_s$$
$$\varphi_s \qquad m_s \cdot \ddot{y}_s \quad \Theta_{sx} \cdot \ddot{\varphi}_s \quad 2d_{by}(\dot{y}_b - \dot{y}_s)$$
$$c_{md}(y_w - y_s) \qquad 2c_{by}(y_b - y_s) \qquad d_m(\dot{y}_w - \dot{y}_s)$$
$$2c_{bz}(z_b - z_s)$$
$$2d_{bz}(\dot{z}_b - \dot{z}_s)$$
$$d_m(\dot{z}_w - \dot{z}_s) \qquad c_{fz} \cdot z_{fR}$$
$$d_{fy} \cdot \dot{y}_{fL} \quad F_L \qquad y_{fR} \quad d_{fz} \cdot \dot{z}_{fR}$$
$$c_{fy} \cdot y_{fL} \qquad d_{fy} \cdot \dot{y}_{fR}$$
$$y_{fL} \quad d_{fz} \cdot \dot{z}_{fL} \qquad c_{fy} \cdot y_{fR} \quad F_R$$
$$z_{fL} \quad c_{fz} \cdot z_{fL} \qquad z_{fR} \qquad \text{d)}$$

Note: The negative vertical displacement in F_L, relating to the coordinate z_{fL}, is considered by the direction of the vertical forces in F_L, so z_{fL} has to be described in the differential equation by: $z_{fL} = -z_s + \varphi_s \cdot b$

Figure 4. Vibration model, cut free into sub-systems

Mass matrix **M**: (15)

$$\mathbf{M} = \begin{bmatrix} m_s & 0 & 0 & 0 & 0 & 0 & 0 & 0 & 0 \\ 0 & m_w & 0 & 0 & 0 & 0 & 0 & 0 & 0 \\ 0 & 0 & m_s & 0 & 0 & 0 & 0 & 0 & 0 \\ 0 & 0 & 0 & m_w & 0 & 0 & 0 & 0 & 0 \\ 0 & 0 & 0 & 0 & \Theta_{sx} & 0 & 0 & 0 & 0 \\ 0 & 0 & 0 & 0 & 0 & 2m_v & 0 & 0 & 0 \\ 0 & 0 & 0 & 0 & 0 & 0 & 2m_b & 0 & 0 \\ 0 & 0 & 0 & 0 & 0 & 0 & 0 & 2m_v & 0 \\ 0 & 0 & 0 & 0 & 0 & 0 & 0 & 0 & 2m_b \end{bmatrix}$$

Damping matrix **D:** (16)

$$\mathbf{D} = \begin{bmatrix} 2(d_{fz} + d_{bz}) + d_m & -d_m & 0 & 0 & 0 & 0 & -2d_{bz} & 0 & 0 \\ -d_m & d_m + d_i & 0 & 0 & 0 & -d_i & 0 & 0 & 0 \\ 0 & 0 & 2(d_{fy} + d_{by}) + d_m & -d_m & -2d_{fy} \cdot h & 0 & 0 & 0 & -2d_{by} \\ 0 & 0 & -d_m & d_m + d_i & 0 & 0 & 0 & -d_i & 0 \\ 0 & 0 & -2d_{fy} \cdot h & 0 & 2(d_{fy}h^2 + d_{fz}b^2) & 0 & 0 & 0 & 0 \\ 0 & -d_i & 0 & 0 & 0 & 2d_{zz} + d_i & -2d_{zz} & 2d_{zy} & -2d_{zy} \\ -2d_{bz} & 0 & 0 & 0 & 0 & -2d_{zz} & 2(d_{zz} + d_{bz}) & -2d_{zy} & 2d_{zy} \\ 0 & 0 & 0 & -d_i & 0 & 2d_{yz} & -2d_{yz} & 2d_{yy} + d_i & -2d_{yy} \\ 0 & 0 & -2d_{by} & 0 & 0 & -2d_{yz} & 2d_{yz} & -2d_{yy} & 2(d_{yy} + d_{by}) \end{bmatrix}$$

Stiffness matrix **C**: (17)

$$
\mathbf{C} = \begin{bmatrix}
2(c_{fz}+c_{bz})-c_{md} & c_{md} & 0 & 0 & 0 & 0 & -2c_{bz} & 0 & 0 \\
c_{md} & c-c_{md} & 0 & \Omega d_i & 0 & -c & 0 & -\Omega d_i & 0 \\
0 & 0 & 2(c_{fy}+c_{by})-c_{md} & c_{md} & -2c_{fy}h & 0 & 0 & 0 & -2c_{by} \\
0 & -\Omega d_i & c_{md} & c-c_{md} & 0 & \Omega d_i & 0 & -c & 0 \\
0 & 0 & -2c_{fy}h & 0 & 2(c_{fy}h^2+c_{fz}b^2) & 0 & 0 & 0 & 0 \\
0 & -c & 0 & -\Omega d_i & 0 & 2c_{zz}+c & -2c_{zz} & 2c_{zy}+\Omega d_i & -2c_{zy} \\
-2c_{bz} & 0 & 0 & 0 & 0 & -2c_{zz} & 2(c_{zz}+c_{bz}) & -2c_{zy} & 2c_{zy} \\
0 & \Omega d_i & 0 & -c & 0 & 2c_{yz}-\Omega d_i & -2c_{yz} & 2c_{yy}+c & -2c_{yy} \\
0 & 0 & -2c_{by} & 0 & 0 & -2c_{yz} & 2c_{yz} & -2c_{yy} & 2(c_{yy}+c_{by})
\end{bmatrix}
$$

Due to the non-symmetric stiffness matrix – caused by the oil film and internal material damping of the rotor – and due to a negative electromagnetic damping coefficient d_m, the vibration system will get instable, when the limit of stability is exceeded ($\Omega > \Omega_{stab}$). The limit of vibration stability Ω_{stab} can be derived, by increasing the rotary angular frequency Ω, and analyzing the eigenvalues.

When a real part of one eigenvalue gets zero, the limit of vibration stability is reached. If the rotary angular frequency Ω is increased furthermore, the real part gets positive and the vibration system gets instable. To find the limit of stability, the homogenous differential equation has to be analyzed. To calculate the eigenvalues, the state-space formulation is used here (with $\mathbf{q}_h = \mathbf{q}$; Index h for homogenous):

$$
\underbrace{\begin{bmatrix} \dot{\mathbf{q}}_h \\ \ddot{\mathbf{q}}_h \end{bmatrix}}_{\dot{\mathbf{x}}} = \underbrace{\begin{bmatrix} \mathbf{0} & \mathbf{I} \\ -\mathbf{M}^{-1}\cdot\mathbf{C} & -\mathbf{M}^{-1}\cdot\mathbf{D} \end{bmatrix}}_{\mathbf{A}} \cdot \underbrace{\begin{bmatrix} \mathbf{q}_h \\ \dot{\mathbf{q}}_h \end{bmatrix}}_{\mathbf{x}}
\tag{18}
$$

With the formulation $\mathbf{x} = \hat{\mathbf{x}} \cdot e^{\lambda \cdot t}$, the eigenvalues can be derived from:

$$
\det[\mathbf{A} - \lambda \cdot \mathbf{I}] = 0
\tag{19}
$$

At the limit of stability, the eigenvalue λ of the critical mode gets:

$$
\lambda = \lambda_{stab} = \pm j \cdot \omega_{stab}
\tag{20}
$$

Knowing the eigenvalue λ_{stab}, the critical mode shape at the limit of stability can be derived. The real part of the critical eigenvalue λ_{stab} is zero and the whirling angular frequency ω_F is then identical to ω_{stab}, while the rotor is rotating with Ω_{stab}. It has to be considered, that the coefficients $d_i, d_{bz}, d_{by}, d_{fz}, d_{fy}\; d_m, c_{md}$ are depending on the whirling angular frequency ω_F, which has to be determined.

Referring to Werner (2016) – where a rigid mounted induction motor was investigated –, an iterative solution has to be deduced, according to Fig. 5, for a soft mounted induction motor. First, the coefficients $d_i, d_{bz}, d_{by}, d_{fz}, d_{fy}, d_m$ and c_{md}, which depend on the whirling angular frequency ω_F, are set to zero, so that only the non-symmetric stiffness matrix of the oil film will cause instability. The eigenvalues are calculated according to (19), depending on the rotary angular frequency Ω.

To derive the limit of stability, the rotary angular frequency Ω is increased, till the real part of an eigenvalue gets zero. At this limit, the rotary angular frequency is $\Omega_{stab,1}$ – index "1" for the first calculation – and the natural angular frequency of the critical mode $\omega_{stab,1}$ can be derived from the eigenvalue. Afterwards the coefficients $d_i, d_{bz}, d_{by}, d_{fz}, d_{fy}, d_m$ and c_{md} are calculated with $\omega_F = \omega_{stab,1}$, and the limit of stability and the natural angular frequency are calculated again, leading to $\Omega_{stab,2}$ and $\omega_{stab,2}$. Then the new calculated natural angular frequency $\omega_{stab,2}$ will be compared to the origin natural angular frequency $\omega_{stab,1}$. If the ratio is less than Δ – an arbitrarily chosen value –, the calculation is finished and $\Omega_{stab} = \Omega_{stab,2}$ and $\omega_{stab} = \omega_{stab,2}$. If the ration is larger as the chosen value Δ, a new calculation is deduced and the coefficients $d_i, d_{bz}, d_{by}, d_{fz}, d_{fy}, d_m$ and c_{md} are now calculated with $\omega_F = \omega_{stab,2}$. With these new coefficients, the new limit of stability $\Omega_{stab,n+1}$ and the natural angular frequency $\omega_{stab,n+1}$ are derived. Then again the new value $\omega_{stab,n+1}$ is compared to the previous value $\omega_{stab,2}$. If the deviation is still too large, the loop in Fig. 5 will run through, till the deviation is less than Δ. With this iterative process the limit of stability Ω_{stab} can be derived, as well as the corresponding natural angular frequency ω_{stab} of the critical mode. This procedure is useful, if the biggest influence on the limit of stability is cau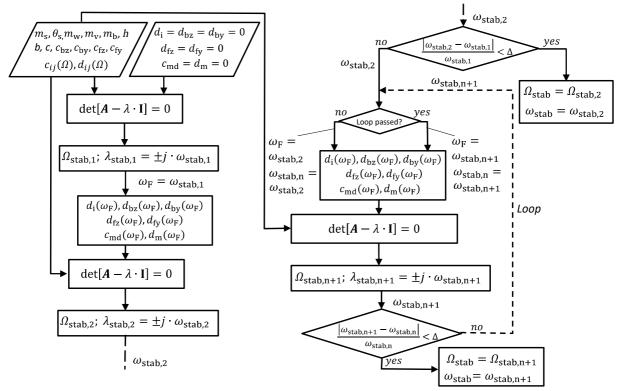sed by the non-symmetric stiffness matrix of the oil film, which is usually the case for common induction motors with sleeve bearings.

Figure 5. Flow diagram to derive the limit of stability for a soft mounted induction motor

5   Numerical Example

The limit of vibration stability for a 2-pole induction motor (Table 1), mounted on soft rubber elements, and driven by a converter with constant magnetization, is analyzed. The load machine is a pump and therefore the load torque is a quadratic function of the rotor speed n. At rated speed, the load torque is identical to the rated torque of the motor.

Table 1. 2-pole induction motor, mounted on soft rubber elements

Data of the motor:	
- Rated power	$P_N = 2400$ kW
- Rated voltage	$U_N = 4160$ V (Δ)
- Rated frequency	$f_N = 60.15$ 1/s
- Rated speed	$n_N = 3600$ rpm
- Rated torque	$M_N = 6366$ Nm
- Rated slip	$s = 0.0025$
- Number of pole pairs	$p = 1$
- Undamped magnetic spring constant	$c_m = 7.0 \cdot 10^6$ kg/s^2
- Masse of the stator	$m_s = 7040$ kg
- Mass inertia of the stator at the *x*-axis	$\theta_{sx} = 1550$ kgm^2
- Mass of the rotor	$m_w = 1900$ kg
- Mass of the rotor shaft journal	$m_v = 10$ kg
- Mass of the bearing housing	$m_b = 80$ kg
- Stiffness of the rotor	$c = 1.8 \cdot 10^8$ kg/s^2
- Height of the centre of gravity S	$h = 560$ mm
- Distance between motor feet	$2b = 1060$ mm
- Horizontal stiffness of bearing housing and end shield	$c_{by} = 4.8 \cdot 10^8$ kg/s^2
- Vertical stiffness of bearing housing and end shield	$c_{bz} = 5.7 \cdot 10^8$ kg/s^2
- Mechanical loss factor of the bearing housing and end shield	$\tan \delta_b = 0.04$
- Mechanical loss factor of the rotor	$\tan \delta_i = 0.03$
Data of the sleeve bearings:	
- Bearing shell	Cylindrical
- Lubricant viscosity grade	ISO VG 32
- Nominal bore diameter / Bearing width	$d_b = 100$ mm / $b_b = 81.4$ mm

- Ambient temperature / Supply oil temperature	$T_{amb} = 20°C$ / $T_{in} = 40°C$
- Mean relative bearing clearance (DIN 31698)	$\Psi_m = 1.6$ ‰
Data of the foundation elements (for each motor side):	
- Vertical stiffness for each motor side	$c_{fz} = 2.0 \cdot 10^7$ kg/s^2
- Horizontal stiffness for each motor side	$c_{fy} = 1.0 \cdot 10^7$ kg/s^2
- Mechanical loss factor of the foundation elements	$\tan \delta_f = 0.1$

The oil film stiffness and damping coefficients of the sleeve bearings have been calculated with the program SBCALC from RENK AG.

First, the coefficients d_i, d_{bz}, d_{by}, d_{fz}, d_{fy}, d_m and c_{md} are set to zero – according to the flow diagram in Figure 5 – and the real part and the imaginary part of the critical eigenvalue is analyzed. The critical vibration mode is the mode, which will get instable (Fig. 6).

Figure 6 shows, that at a rotor speed of 4595 rpm the real part of the critical eigenvalue becomes zero. Increasing the rotor speed, will lead to a positive real part and therefore to instability. So the limit of stability is reached at a rotor speed of $n_{stab,1} = 4595$ rpm ($\Omega_{stab,1} = 481.2$ rad/s).
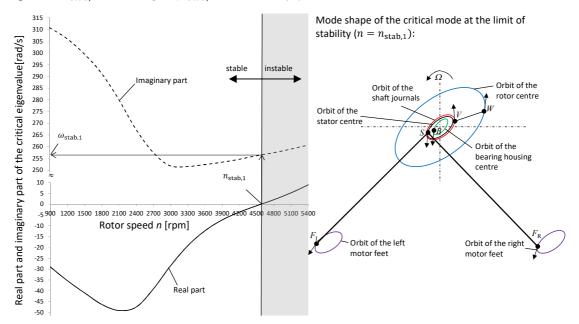

Figure 6. Real and imaginary part of the critical eigenvalue, depending on the rotor speed, with the boundary condition: $d_i = d_{bz} = d_{by} = d_{fz} = d_{fy} = d_m = c_{md} = 0$; Critical mode shape at the limit of stability

At this rotor speed the imaginary part, which represents the whirling angular frequency ω_F of the critical natural mode, becomes $\omega_F = \omega_{stab,1} = 255.3$ rad/s. According to the flow diagram this angular natural frequency $\omega_{stab,1}$ can now be used to calculate the coefficients d_i, d_{bz}, d_{by}, d_{fz}, d_{fy}, d_m and c_{md} (Table 2).

Table 2. Coefficients d_i, d_{bz}, d_{by}, d_{fz}, d_{fy}, d_m and c_{md} at a rotor speed of $n_{stab,1} = 4595$ rpm and at a whirling angular frequency of $\omega_F = \omega_{stab,1} = 255.3$ rad/s

Damping constant of the rotor	$d_i = 2.12 \cdot 10^4$ kg/s
Damping constant of bearing housing and end shield (horizontal direction)	$d_{by} = 7.52 \cdot 10^4$ kg/s
Damping constant of bearing housing and end shield (vertical direction)	$d_{bz} = 8.93 \cdot 10^4$ kg/s
Damping constant of foundation elements for each motor side (horizontal direction)	$d_{fy} = 3.92 \cdot 10^3$ kg/s
Damping constant of foundation elements for each motor side (vertical direction)	$d_{fz} = 7.83 \cdot 10^3$ kg/s
Electromagnetic damping constant	$d_m = -61.7$ kg/s
Electromagnetic spring constant	$c_{md} = 4.82 \cdot 10^5$ kg/s^2

The large difference between rotor angular frequency $\Omega_{stab,1} = 481.2$ rad/s and the whirling angular frequency $\omega_F = \omega_{stab,1} = 255.3$ rad/s, leads in combination with a very small fundamental slip $s = 0.0032$ to a large harmonic slip $s_v = -0.47$, and therefore to a strong electromagnetic field damping, and the electromagnetic coefficients d_m and c_{md} get very small. Fig. 7 shows, that the electromagnetic coefficients would be much higher, if the whirling angular frequency ω_F would be close to the rotor angular frequency Ω.
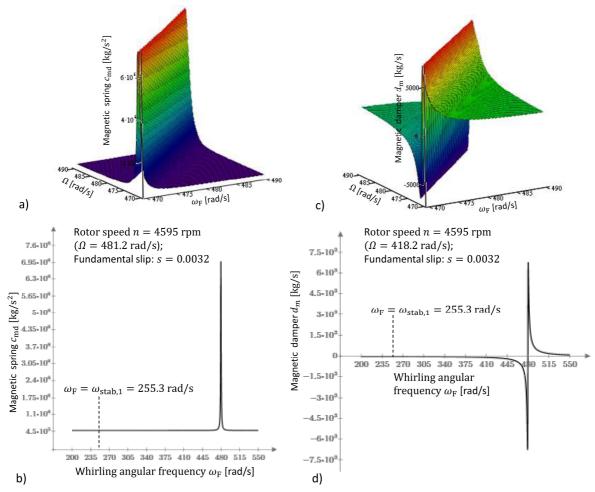
Figure 7. Magnetic spring constant a) and b) and magnetic damper constant c) and d) for different whirling angular frequencies and different rotor angular frequencies

With the basic coefficients from Table 2, the limit of stability is calculated again according to the flow diagram. To clarify this additional calculation, the index "2" is used instead of index "1". So the limit of vibration stability is reached now at a rotor speed of $n_{stab,2} = 4554$ rpm and the whirling frequency is $\omega_F = \omega_{stab,2} = 255.6$ rad/s. According to the flow diagram a third calculation is not necessary, because $\omega_{stab,2}$ differs only marginal from $\omega_{stab,1}$ (+0.12%). Therefore, the values for the limit of stability are $n_{stab} = n_{stab,2} = 4554$ rpm; $\omega_{stab} = \omega_{stab,2} = 255.6$ rad/s. Now different cases are investigated. Table 3 shows, that the electromagnetic damper d_m and the electromagnetic spring constant c_{md} influence the limit of vibration stability only marginal (case b and c), because the large harmonic slip at the limit of stability causes a strong electromagnetic field damping and therefore leading to low values for d_m and c_{md}. Without considering electromagnetic field damping (case d), the magnetic spring value gets maximal ($c_{md} = c_m$) and the magnetic damper coefficient gets zero ($d_m = 0$). For this case, the limit of stability will be clearly reduced from 4554 rpm to 4377 rpm, which means -3.9%. When neglecting the internal damping of the rotor (case e), the limit of stability will be increased (+2.0%).

Table 3. Limit of stability for different cases

Case	Description	ω_{stab} [rad/s]	n_{stab} [rpm]	Δ of n_{stab} to a) [%]
a)	Data Table 2 (Basic conditions)	255.6	4554	0
b)	Data Table 2 with $d_m = 0$	256.5	4556	+0.04
c)	Data Table 2 with $c_{md} = 0$	256.5	4566	+0.26
d)	Data Table 2 with $d_m = 0$; $c_{md} = c_m$ (no electromagnetic field damping)	248.1	4377	-3.9
e)	Data Table 2 with $d_i = 0$ (no internal damping of the rotor)	255.7	4645	+2.0
f)	Data Table 2 with $d_{by} = d_{bz} = 0$ (no damping of the bearing housing and end shield)	256.5	4509	-1.0
g)	Data Table 2 with $d_{fy} = d_{fz} = 0$ (no damping of the foundation elements)	256.1	4537	-0.37
h)	Data Table 2 with $c_{fy} = c_{fz} \to \infty$ (motor rigid mounted)	226.4	3922	-13.9

However, neglecting the damping of the bearing housings and end-shields (case f) will lower the limit of stability (-1%), as well as neglecting the damping of the foundation elements (-0.37%). The low influence of the damping of the foundation elements is caused by their low stiffness, which leads in conjunction with the loss factor to low damping values, which can be seen in Table 2. Figure 8 shows, that if the foundation element stiffness would be e.g. 4 times higher and the mechanical loss factor of the foundation elements would be the same ($\tan \delta_f = 0.1$), the limit of stability would increase from 4554 rpm to 4880 rpm (+7.2%). However, for a low loss factor ($\tan \delta_f = 0.01$) the limit of stability would only increase to 4730 rpm (+3.9%).
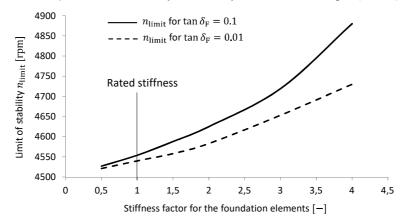

Figure 8. Influence of the foundation element stiffness on the limit of stability n_{limit}

Figure 9 shows the influence on the limit of stability and on the whirling angular frequency ω_{stab}, for stiffness variation of the foundation elements in a range of $c_{fy} = 1 \cdot 10^6 \dots 4 \cdot 10^7 \text{kg/s}^2$; $c_{fz} = 1 \cdot 10^6 \dots 8 \cdot 10^7 \text{kg/s}^2$.
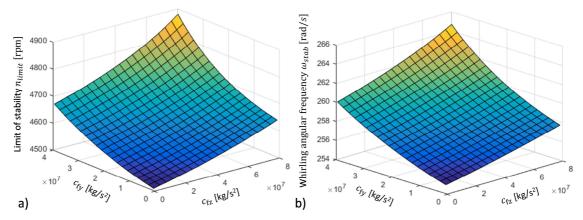

Figure 9. Influence of the arbitrary stiffness of the foundation elements on a) the limit of stability n_{limit} and on b) the whirling angular frequency ω_{stab}; with a loss factor of $\tan \delta_f = 0.1$ for the foundation elements

If the motor would be rigid mounted (case h), which means $c_{fy} = c_{fz} \rightarrow \infty$, the limit of stability would be reached already at 3922 rpm, and the whirling frequency at the limit of stability ω_{stab} would be 226.4 rad/s instead of 255.6 rad/s, shown by Werner (2016). Therefore, putting here the motor on the soft foundation elements increases the limit of stability clearly (+16.1%), compared to the rigid mounted induction motor.

6 Conclusion

In the paper a multibody vibration model and a procedure are presented for stability analysis of soft mounted induction motors, with sleeve bearings. The focus of the paper is on the influence of electromagnetic field damping, regarding the limit of stability. After the mathematical coherences have been derived, a numerical example was presented, where the limit of stability was analyzed. It could be shown, that neglecting electromagnetic field damping leads to a lower limit of stability. Additionally the influence of the foundation elements and of the internal damping of the rotor on the limit of stability could be demonstrated. Although, the vibration model is a simplified multibody model, the procedure and conclusions can be adopted into finite-element analysis.

References

Arkkio, A.; Antila, M.; Pokki, K.; Simon, A.; Lantto, E.: Electromagnetic force on a whirling cage rotor. *Electr. Power Appl.*, Vol. 147, No. 5, (2000), 353-360.

Früchtenicht, J.; Jordan, H.; Seinsch, H.O.: Exzentrizitätsfelder als Ursache von Laufinstabilitäten bei Asynchronmaschinen. *Archiv für Elektrotechnik*, Vol. 65, Issue 4, Part 1, pp. 271-281, Part 2, (1982), 283-292.

Gasch, R.; Maurer J.; Sarfeld, W.: The influence of the elastic half space on stability and unbalance of a simple rotor-bearing foundation system, *Conference Vibration in Rotating Machinery*, C300/84, IMechE, Edinburg, (1984), 1-12.

Gasch, R.; Nordmann, R.; Pfützner H.: *Rotordynamik*. Springer-Verlag, Berlin-Heidelberg, (2002).

Genta, G.: *Dynamics of Rotating Systems*. Springer Science & Business Media, (2005).

Glienicke, J.: *Feder- und Dämfpungskonstanten von Gleitlagern für Turbomaschinen und deren Einfluss auf das Schwingungsverhalten eines einfachen Rotors*. Dissertation TH Karlsruhe, (1966).

Holopainen, T.P.: *Electromechanical interaction in rotor dynamics of cage induction motors*. VTT Technical Research Centre of Finland, Ph. D. Thesis, Helsinki University of Technology, Finland, (2004).

Kirk, R.G.; DeChowdhury, P.; Gunter, E.J.: The effect of support flexibility on the stability of rotors mounted in plain cylindrical bearings, *IUTAM Symposium Dynamics of Rotors*, (1974), 244-298.

Lund, J.; Thomsen, K.: *A calculation method and data for the dynamics of oil lubricated journal bearings in fluid film bearings and rotor bearings system design and optimization*, ASME, New York, (1978), 1-28.

Rao, J. S.: *Rotor Dynamics*. New Age International, (1996).

Schuisky, W.: Magnetic pull in electrical machines due to the eccentricity of the rotor. *Electrical Research Association Trans.* 295, (1972), 391-399.

Seinsch, H.-O.: *Oberfelderscheinungen in Drehfeldmaschinen*. Teubner-Verlag, Stuttgart, (1992).

Smith, A.C.; Dorrell, D.G.: Calculation and measurement of unbalanced magnetic pull in cage induction motors with eccentric rotors. I. Analytical model. *Electric Power Applications.* Vol. 143, Issue 3, (1996), 193–201.

Tondl, A.: *Some Problems of Rotordynamics*. Chapman and Hall, London, (1965).

Werner, U.: *Rotordynamische Analyse von Asynchronmaschinen mit magnetischen Unsymmetrien*. Dissertation, Technical University of Darmstadt, (2006).

Werner, U.: Vibration stability of soft mounted asynchronous machines with flexible shafts and sleeve bearings considering electromagnetic effects. *ISMA 23rd International Conference on Noise & Vibration Engineering*, Leuven, Belgium, 15-17 September, (2008), 1167-1182.

Werner, U.: Stability analysis of induction rotors supported in sleeve bearings considering electromagnetic field damping and internal material damping of the rotor. *Vibration in rotating machinery*, Manchester, UK, Sept. 13-15, (2016), 155-166.

Address: Georg Simon Ohm University of Applied Sciences Nuremberg, Keßlerplatz 12, 90489 Nuremberg, Germany

email: ulrich.werner@th-nuernberg.de